Low-lying neutron *fp*-shell intruder states in ^{27}Ne

S.M. Brown,[1] W.N. Catford,[1] J. S. Thomas,[1] B. Fernández-Domínguez,[2,3] N. A. Orr,[2] M. Labiche,[4] M. Rejmund,[5] N.L. Achouri,[2] H. Al Falou,[2] N. I. Ashwood,[6] D. Beaumel,[7] Y. Blumenfeld,[7] B. A. Brown,[8] R. Chapman,[9] M. Chartier,[3] N. Curtis,[6] G. de France,[5] N. de Sereville,[7] F. Delaunay,[2] A. Drouart,[10] C. Force,[5] S. Franchoo,[7] J. Guillot,[7] P. Haigh,[6] F. Hammache,[7] V. Lapoux,[10] R. C. Lemmon,[4] A. Leprince,[2] F. Maréchal,[7] X. Mougeot,[10] B. Mouginot,[7] L. Nalpas,[10] A. Navin,[5] N. P. Patterson,[1] B. Pietras,[3] E. C. Pollacco,[10] A. Ramus,[7] J. A. Scarpaci,[7] I. Stefan,[7] and G. L. Wilson[1]

[1]*Faculty of Engineering and Physical Sciences, University of Surrey, Guildford, GU2 7XH, UK*
[2]*LPC-Caen, ENSICAEN, Université de Caen, CNRS/IN2P3, 14050 Caen Cedex, France*
[3]*Oliver Lodge Laboratory, School of Physical Sciences, University of Liverpool, Liverpool L69 7ZE, UK*
[4]*Nuclear Structure Group, STFC Daresbury Laboratory, Daresbury, Warrington WA4 4AD, UK*
[5]*GANIL, BP 55027, 14076 Caen Cedex 5, France*
[6]*School of Physics and Astronomy, University of Birmingham, Birmingham B15 2TT, UK*
[7]*IPN-Orsay, 91406 Orsay, France*
[8]*NSCL and Department of Physics and Astronomy, Michigan State University, East Lansing, MI 48824, USA*
[9]*SUPA, School of Engineering, University of the West of Scotland, Paisley PA1 2BE, UK*
[10]*CEA-Saclay, IRFU/Service de Physique Nucléaire, 91191 Gif-sur-Yvette, France*

(Dated: January 11, 2012)

The quenching of the N=20 shell gap in neutron-rich nuclei is investigated by studying the single-particle structure of ^{27}Ne via neutron transfer using a ^{26}Ne beam. Two low-lying negative parity intruder states have been observed, the lowest of which is identified as $J^\pi = 3/2^-$, confirming earlier speculations. A level identified as $7/2^-$ is observed higher in energy than the $3/2^-$, contrary to the ordering at β-stability and at an energy significantly different to the predictions of previous shell-model calculations. The measured energies and deduced spectroscopic factors are well reproduced in full (0,1)-$\hbar\omega$ 0*s*-0*p*-0*d*-1*s*-0*f*-1*p* calculations in which there is a significant ad-hoc reduction ($\sim$ 0.7 MeV) in the N=20 shell gap.

PACS numbers: 21.10.Jx; 21.60.Cs; 24.50.+g; 25.60.Je

Neutron-rich nuclei often exhibit structural behaviour significantly different to stable nuclei, with a striking example being the "island of inversion" in the $A \simeq 32$ region of neutron rich nuclei [1, 2]. The nuclei in this "island" are deformed rather than spherical owing to residual interactions and quenching of the N=20 magic number through the migration in energy of the shell-model orbitals [3]. This migration is known to be due, in part, to nucleon-nucleon tensor forces and to three-body NNN forces [4, 5]. In adjacent more weakly bound nuclei, the migration may also be affected by the proximity of the continuum [6].

The N=20 shell gap seen in nuclei near stability arises from the separation of the $0d_{3/2}$ orbital and the negative parity orbitals ($0f_{7/2}$, $1p_{3/2}$,...) of the next major shell. A sudden collapse of this gap is observed when going from ^{31}Si to ^{29}Mg [7, 8] (a removal of two protons from the $0d_{5/2}$ orbital) whereby low-lying negative parity states appear in ^{29}Mg. In addition, the lowest $7/2^-$ and $3/2^-$ states appear to be reordered, compared to nuclei closer to stability [8]. These effects have been confirmed in the N=15 nucleus ^{25}Ne [9] but cannot be reproduced quantitatively by any existing shell-model calculations.

Recent experiments investigating ^{27}Ne have identified two bound states above the $3/2^+$ ground state. A level at 765 keV with significant single-particle strength was observed via d(^{26}Ne,^{27}Ne γ)p together with a very weak level at 885 keV [10]. Guided by shell model expectations, the 885 keV level was tentatively identified as the lowest $1/2^+$ state and the 765 keV level was inferred to have a negative parity of $1/2^-$, $3/2^-$ or $5/2^-$. The $1/2^+$ is weak since it is populated mainly via pair-excited components in the ^{26}Ne ground state, in single-step transfer. In single-neutron knockout at higher energies, both levels were seen and the angular momentum of the removed nucleon was assigned as ℓ=0 or 1 [11], consistent with the results from the (d,p) reaction study [10]. These two excited states were also observed in the p(^{28}Ne,^{27}Neγ) reaction at intermediate energy [12] but no further information concerning spins was obtained [37]. No evidence for a $7/2^-$ state has been reported, despite a clear prediction that it should exist at an energy close to the $3/2^-$ state [11, 15]. The most direct means to probe the evolution of orbital energies is to measure the strength of single-particle states where a neutron is transferred into orbitals that are otherwise empty. The present experiment was designed along these lines to populate the $7/2^-$ and $3/2^-$ $0f$-$1p$ shell states and any other strong single-particle levels via (d,p) transfer and to determine their properties.

A beam of ^{26}Ne ions ($\sim$100% pure) at 9.8A MeV was provided by the SPIRAL facility at GANIL and

used to bombard a $(CD_2)_n$ target of measured thickness 1.20 mg/cm^2. The beam intensity was ∼2500 particles/sec. The TIARA silicon array [16], which covered 76% of 4π over laboratory angles from 36° - 169°, was employed to detect the protons. The angles from 36° - 144° were spanned by an octagonal "barrel" of detectors and the angles 144° - 169° were covered by an annular array. Four segmented EXOGAM Ge clover detectors [17], located at 90°, surrounded the target at a distance of 54 mm. The photopeak efficiency for γ-ray detection was 10(1)% at 800 keV. Identification of the beam-like reaction products was achieved by measuring their trajectory, energy loss and time of flight using the VAMOS magnetic spectrometer [18]. A detailed description of the set-up may be found in Ref. [16].

Elastically scattered deuterons were detected forward of 90° [19] in coincidence with ^{26}Ne events in VAMOS. As in our earlier experiments [9, 20] the normalisation of the differential cross sections was obtained by fitting the deuteron elastic scattering data to optical model calculations using parameters from Ref. [21]. Protons from the (d,p) reaction populating bound states in ^{27}Ne were selected by requiring a ^{27}Ne coincidence in VAMOS. The measurements of the energy and angle of the protons in TIARA were used to calculate the excitation energy in ^{27}Ne.

The excitation energy resolution at backward angles, where the proton energy was lowest, was limited by the proton energy loss in the target. According to simulations using GEANT4 [22], the 1.20 mg/cm^2 target limited the excitation energy resolution to 630 keV (FWHM) at the backward angles. The resolution was worse (∼ 1 MeV) at the forward angles where the limitation was due to the protons not being stopped [23]. Thus, it was not possible to resolve the bound states in ^{27}Ne using only the data recorded with TIARA and a gate on the γ-rays measured in EXOGAM was necessary to select individual states. Figure 1 shows the Doppler corrected EXOGAM spectrum in coincidence with ^{27}Ne. The peak measured at 767(2) keV corresponds to the decay of the $3/2^-$ level at 765 keV, while the counts observed at 894(13) keV arise from the $1/2^+$ state at 885 keV [10, 11].

The spectroscopic factor of the 765 keV state was deduced by scaling a theoretical calculation (see below) to the proton angular distribution obtained by gating on the 765 keV γ-ray transition. The data were corrected for the γ-ray photopeak efficiency in EXOGAM, the Lorentz boost to the γ-ray angular distribution ($\beta(^{27}\mathrm{Ne}) = 0.13c$) and the geometric efficiency of TIARA. The correction for the γ-ray efficiency is the same for each proton angle bin if the γ-rays are emitted isotropically (as is the case for decays of the $1/2^+$ state at 885 keV). In general, the γ-ray distribution is anisotropic and the details depend on the multipolarity of the radiation and on the magnetic substate populations of the level. These vary with proton angle. Reaction cross sections were calculated using the Adiabatic Distorted Wave Approximation (ADWA) method [24] for zero range with standard parameters that have been demonstrated to produce spectroscopic factors consistent with large-basis shell-model calculations [25]. The CH89 [27] phenomenological nucleon-nucleus optical potentials were used for the $n + p$ system in the incident channel and the proton in the exit channel [25]. Using the calculated magnetic substate distributions and the formalism of Ref. [28], deviations of up to 15% in the coincidence efficiency (relative to isotropic γ-emission) were calculated for individual proton angle bins [23]. This correction for the γ-ray efficiency is intrinsically dependent on the assumed spin in ^{27}Ne. Figure 2 shows the 765 keV γ-ray gated data with efficiency corrections calculated assuming four different spins for the final state in ^{27}Ne. Proton bins of equal width in laboratory angle were employed in the regions 35°-85°, 95°-135° and 150°-165°. The best fit is for the $3/2^-$ ADWA calculation, with a spectroscopic factor of 0.64(33). The error of ∼50% is dominated by the limited statistics for this p-γ coincidence data. The next best fit is for ℓ=2 but the presence of a second $3/2^+$ state, or indeed a strong $5/2^+$ state, so close to the ground state is contrary to any theoretical expectations. Thus, a spin of $3/2^-$ was deduced for the 765 keV state.

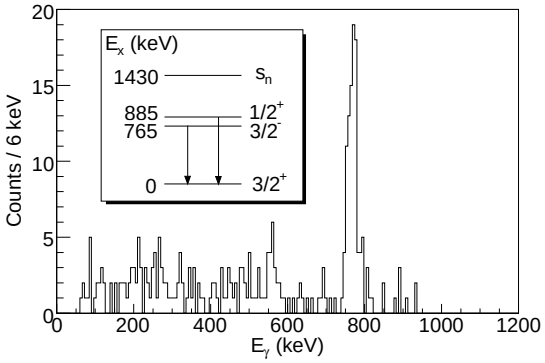

FIG. 1: Doppler corrected energy spectrum of γ-rays measured in coincidence with ^{27}Ne. The strong peak corresponds to de-excitation of the $3/2^-$ state at 765 keV, whilst the counts around 890 keV arise from the $1/2^+$ state at 885 keV. The Compton edge of the 765 keV peak is at 573 keV.

The γ-ray statistics for the 885 keV $1/2^+$ state gave an uncertainty of more than 80% in the magnitude of the (d,p) yield and a spectroscopic factor of 0.17(14) was deduced [23]. The spectroscopic factors for both bound excited states are in agreement with previous measurements (Table I). The quoted errors include contributions from counting statistics, an absolute normalisation uncertainty of 10% and an estimated 20% uncertainty in the reaction modelling (including ∼ 15% variation between calculations employing Becchetti-Greenlees [26] or Chapel Hill [29] nucleon-nucleus potentials in the

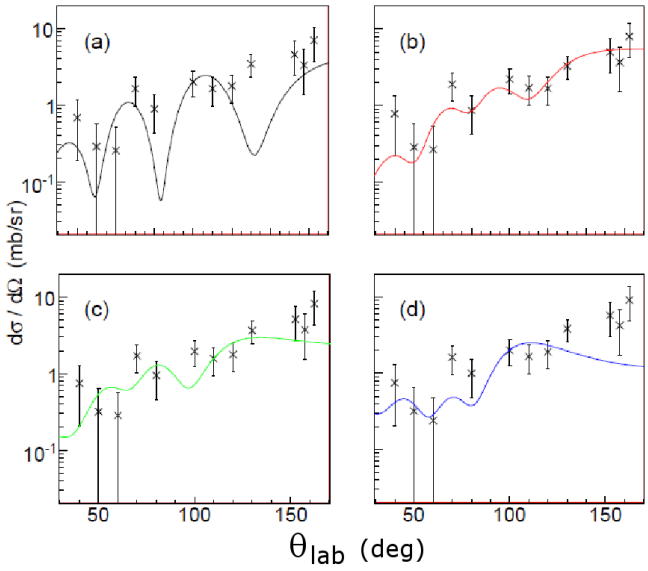

FIG. 2: (Color on-line) Proton angular distributions gated on 765 keV gamma rays, corrected for gamma-ray coincidence efficiency according to different assumptions for the final state (see text): a) J^π=1/2$^+$ (ℓ=0), b) 3/2$^-$ (ℓ=1), c) 3/2$^+$ (ℓ=2), d) 7/2$^-$ (ℓ=3). A transfer of ℓ=1 is deduced.

ADWA). For the 1/2$^+$ and 3/2$^-$ states, the errors also include a 10% uncertainty in the γ-ray photopeak coincidence efficiency.

In order to study the ground state angular distribution, a gate on excitation energy (E_x < 200 keV) was used to exclude the known bound excited states. The corresponding angular distribution for ^{27}Ne coincidences showed a clear signature for $\ell = 2$ transfer [23]. Further, if the 765 keV and 885 keV yields (after correcting for the γ-ray efficiency) are subtracted from the total proton yield in coincidence with ^{27}Ne, the resulting angular distribution is best reproduced by a 3/2$^+$ (ℓ=2) calculation. This gives a spectroscopic factor for the ground state of 0.42(22), in agreement with the previous transfer measurement [10] (Table I). Therefore, no bound states other than those observed are required by the present data. This conclusion is supported by the shell-model calculations, discussed below, that best describe all of the states seen here.

Protons from (d,p) reactions to unbound states in ^{27}Ne were also observed, in coincidence with ^{26}Ne in VAMOS. In the region forward of 90° in the laboratory, protons arising from d(^{26}Ne,p) could be distinguished from the protons and deuterons arising from elastic scattering (both present in the target) by evaluating the missing momentum. That is, the combined momentum of the light ejectile recorded in TIARA and the recoil in VAMOS was compared to that of the incident beam. For ^{27}Ne* $\rightarrow$^{26}Ne+n, the momentum of the undetected neutron was sufficiently well defined to resolve these events from elastic scattering [23]. The energies of protons populating unbound states in ^{27}Ne were below the discriminator thresholds in the annular array, so only data from the barrel were used.

A background arising from direct breakup to the ^{26}Ne+n+p three-body final state may in principle contribute to the spectra for the d(^{26}Ne,p)^{27}Ne* $\rightarrow$ ^{26}Ne+n channel. As detailed in Ref. [23], this contribution was simulated by randomly sampling the available three-body phase space and including experimental resolutions and the same sorting restrictions as applied to the data. The simulated breakup contribution was scaled so that it did not exceed the observed yield at any angle. As expected, the breakup contribution was largest at forward laboratory angles and negligible at backward angles (Figure 3). The data exhibit an isolated peak at 1.74(9) MeV. Additional counts at higher energy could represent a single state or indeed the combined contributions of many. However, the effect of the detection thresholds in the TIARA barrel is to progressively exclude counts for E_x > 4 MeV, giving the appearance of a peak. This progressive cut-off is also present in the forward angle data, but the kinematics dictate that the low proton energy threshold corresponds to higher excitation energies for these angles. The width of the peak at 1.74 MeV was dominated by the experimental resolution, which was obtained from simulations (FWHM = 0.95 MeV for Figure 3(b)) [23]. A Gaussian of this width was convolved with a Breit-Wigner shape for which the width was a fitted parameter, with the result that Γ was consistent with zero and Γ < 0.46 MeV (2σ limit). The angular distribution is shown in Figure 4, where the uncertainties include those arising from the normalisation of the direct breakup contribution. Proton bins of equal width in laboratory angle were employed in the regions 45°-75° and 100°-140°. Importantly, the apparent higher energy peak does not have an appreciable effect on the angular distribution.

Through comparison with ADWA calculations (Figure 4), the transferred angular momentum for the 1.74 MeV state was deduced to be $\ell = 3$. The calculations employed the method of Vincent and Fortune [29, 30] for unbound states. An alternative analysis using a "slightly bound" form factor [31] gives essentially identical results. From a shell-model perspective (see below), the lowest lying $\ell = 3$ state (by at least 1 MeV) is predicted to be the first 7/2$^-$ level as driven primarily by the single particle energies. A 7/2$^-$ assignment is thus inferred and, as such, a spectroscopic factor of 0.35(10) deduced. The method of Vincent and Fortune gives the natural width of the state to be 3.5(10) keV, which is negligibly small compared to the experimental resolution.

Figure 5 displays the experimental ^{27}Ne level scheme compared to shell-model calculations. The SDPF-M [15] interaction, in which the monopole matrix elements were modified to produce the drip line for the oxygen isotopes, fails completely in reproducing the energy of the 7/2$^-$

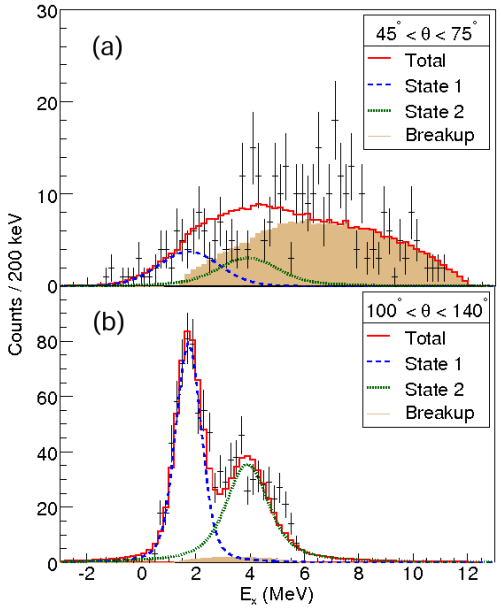

FIG. 3: (Color on-line) Excitation energy spectra in the (a) forward and (b) backward angular regions of the barrel. The fits included Gaussians peaks (see text) and a contribution from direct breakup (shaded).

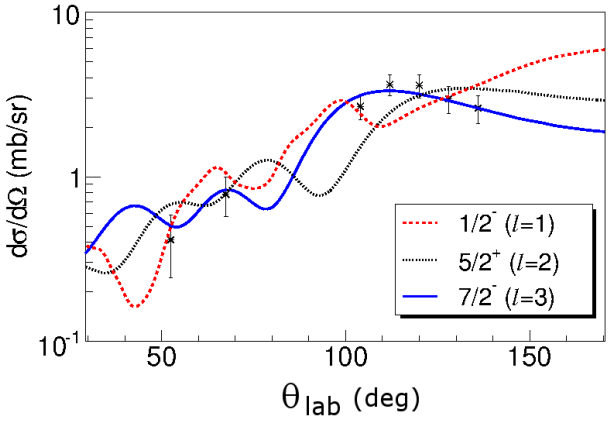

FIG. 4: (Color on-line) Proton angular distribution for the unbound state at 1.74 MeV excitation energy, compared to ADWA theory. The J^π values used for different ℓ follow simple shell-model expectations. Error bars are statistical only.

state. Furthermore, the ordering of the negative parity states is not predicted correctly. This follows a similar failure for ^{25}Ne [9, 11] and the isotone ^{29}Mg [8].

In Ref. [32] the WBP Hamiltonian was developed for the mass region A=10-20 in the $0s$-$0p$-$0d$-$1s$-$0f$-$1p$ model space. The $1s$-$0d$ part of the interaction is the USD Hamiltonian [33]. The data considered in Ref. [32] were mainly for configurations dominated by the $0p$, $0d$ and $1s$ orbitals. The $0f$-$1p$ shell was added in order to account for spurious states. As discussed in Ref. [32], the $1p_{3/2}$ single-particle energy was determined from the strength

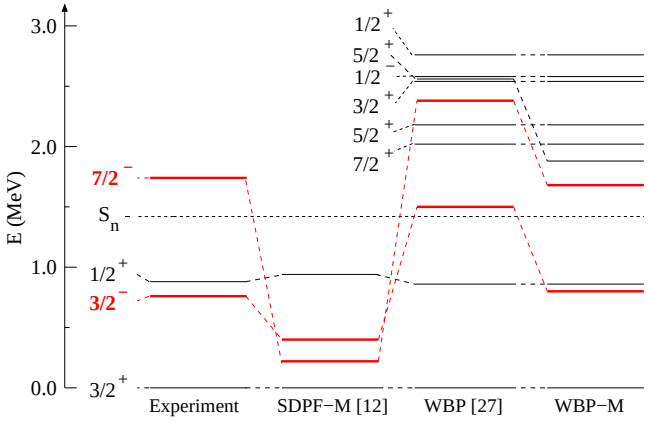

FIG. 5: (Color on-line) Level scheme for ^{27}Ne. The measurements (Table I) are compared to shell-model calculations using different interactions, including the WBP-M which incorporates a shift of −0.7 MeV (see text).

TABLE I: Comparison between experimental and calculated (see text) excitation energies and spectroscopic factors for states in ^{27}Ne. Experimental excitation energies are from [10] except for the 1.74 MeV state (present work). For C^2S, the errors include uncertainties from the reaction model.

J^π	E^*_{exp}	E^*_{WBP-M}	C^2S		
	(MeV)	(MeV)	Ref. [10]	Present	WBP-M
$3/2^+$	0	0	0.2(2)	0.42(22)	0.63
$3/2^-$	0.765	0.809	0.6(2)	0.64(33)	0.67
$1/2^+$	0.885	0.869	0.3(1)	0.17(14)	0.17
$7/2^-$	1.74	1.686	-	0.35(10)	0.40

distribution of 2^- states in the ^{19}F(d,p)^{20}F reaction, and the $0f_{7/2}$ single-particle energy was determined from the strength distribution of 6^- states in the ^{20}Ne(p,n)^{20}Na reaction. The WBP calculations presented in this work allowed for a maximum of $1\hbar\omega$ excitations across a shell gap. Therefore, positive parity states are simply USD calculations. When the WBP interaction is used for ^{27}Ne, the lowest $3/2^-$ and $7/2^-$ states have configurations that are dominated by one neutron occupying the $1p_{3/2}$ and $0f_{7/2}$ orbitals, respectively. Although the ordering of the negative parity states is reproduced, the energies of these states are about 0.7 MeV too high compared to the present experiment (Figure 5). We have, therefore, implemented calculations employing a modified WBP Hamiltonian (WBP-M) in which the energies of the $0f$-$1p$ shell orbitals are lowered relative to the $1s$-$0d$ shell. The level scheme for ^{27}Ne with a lowering of 0.7 MeV is shown in Figure 5 and the spectroscopic factors are given in Table I. The WBP and WBP-M calculations give essentially identical spectroscopic factors whilst the latter better reproduces the excitation energies of the negative parity states.

Comparison was also made for these states in the adjacent nuclei ^{25}Ne and ^{29}Mg. The ordering of the nega-

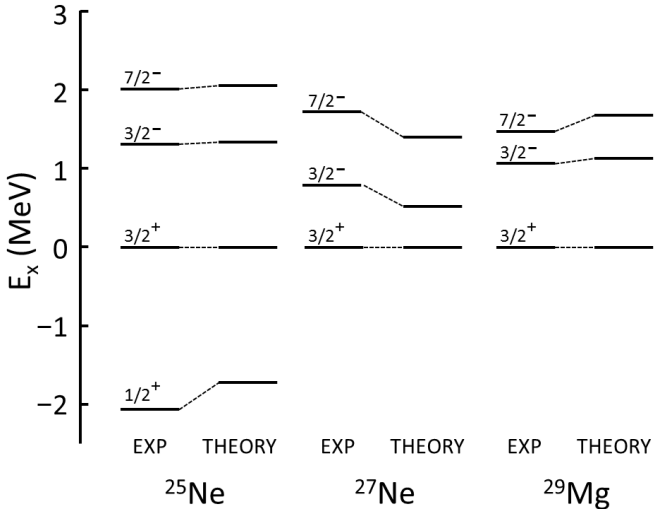

FIG. 6: Experimental and theoretical energies, relative to the $3/2_1^+$ level, of the $0f$-$1p$ states in the region of ^{27}Ne. The shell model calculations employed the WBP-M interaction with a shift of −1.0 MeV (see text).

tive parity states was again correctly predicted with the WBP Hamiltonian, but a shift of −1.0 MeV was required to reproduce the excitation energies (in ^{29}Mg) and the spacing between the $3/2_1^+$ and the negative parity states (in ^{25}Ne), as shown in Figure 6. The spectroscopic factors were again essentially unchanged by the energy shift. Since the $3/2_1^+$ lies higher than the USD prediction (by $\sim$ 0.3 MeV) in ^{25}Ne [9], this effect may account for up to half of the level shift applied in the WBP-M interaction. Relative to ^{27}Ne, the addition of two protons (^{29}Mg) reduces the experimentally observed gap between the $3/2^-$ and $7/2^-$ states from 975 keV to 336 keV. The removal of two neutrons (^{25}Ne) reduces the gap to 700 keV. In the more exotic nucleus ^{31}Mg, the gap reduces to just 240 keV [35]. The WBP-M prediction is 603 keV, whilst the *sd-pf* calculations of Ref. [35], finely tuned to ^{31}Mg, predict 150 keV. The WBP-M calculations cannot, however, be used to extend the Figure 6 systematics to include ^{31}Mg, as the low-lying positive parity states (including the $3/2_1^+$) are dominated by $2p$-$2h$ configurations [35] which are beyond the scope of the present model.

In summary, the N=20 shell gap in neutron-rich nuclei has been investigated by studying the single-particle strength in ^{27}Ne. In particular, the lower of two intruder states, at 765 keV, has been identified as $3/2^-$ which confirms earlier conjectures [10, 11]. The $7/2^-$ intruder state has been located at an excitation energy of 1.74(9) MeV, 0.33(9) MeV above the neutron emission threshold. Thus the $7/2^-$ state is higher in energy than the $3/2^-$ state, contrary to the ordering at β-stability. This is, however, consistent with the ordering in the N=17 isotone ^{29}Mg [8] and the N=15 isotones ^{25}Ne [9] and ^{27}Mg [34]. The SDPF-M interaction is unable to reproduce the energies or ordering of these negative parity states. Using the WBP interaction, with the single-particle energies of the $0f$-$1p$ shell lowered so as to reduce the N=20 gap by 0.7 MeV, the shell-model predicts the energies and spectroscopic factors of the states in ^{27}Ne remarkably well. A slightly larger reduction of 1.0 MeV is required for the adjacent nuclei ^{25}Ne and ^{29}Mg. It would be interesting to develop a new interaction that would succeed in reducing the effective gap between the $0d_{3/2}$ orbital and the $0f$-$1p$ shell in a natural way, without the need for ad-hoc changes. Finally, the investigation of the present results using models which include explicitly the continuum would be welcome [36].

The authors thank N. Timofeyuk for useful discussions and E.C. Simpson for assistance with shell model calculations. The excellent support provided by the technical staff of LPC and GANIL is also acknowledged. This work was supported by STFC grant PP/F000715/1 and NSF grant PHY-0758099.

[1] C. Thibault *et al.*, Phys. Rev. C **12**, 164 (1975).
[2] see, for example, E.K. Warburton *et al.*, Phys. Rev. C **41**, 1147 (1990); E. Caurier *et al.*, Rev. Mod. Phys. **77**, 427 (2005) and references therein.
[3] O. Sorlin and M. G. Porquet, Prog. Part. Nucl. Phys. **61**, 602 (2008).
[4] T. Otsuka *et al.*, Phys. Rev. Lett. **105**, 032501 (2010).
[5] J.D. Holt *et al.*, arXiv:1009.5984v1 [nucl-th].
[6] J Dobaczewski *et al.*, Prog. Part. Nucl. Phys. **59**, 432 (2007).
[7] B.H. Wildenthal and P.W.M. Glaudemans, Nucl. Phys. A **108**, 49 (1968).
[8] J.R. Terry *et al.*, Phys. Rev. C **77**, 014316 (2008).
[9] W.N. Catford *et al.*, Phys. Rev. Lett. **104**, 192501 (2010).
[10] A. Obertelli *et al.*, Phys. Lett. B **633**, 33 (2006).
[11] J.R. Terry *et al.*, Phys. Lett. B **640**, 86 (2006).
[12] Z. Dombrádi *et al.*, Phys. Rev. Lett. **96**, 182501 (2006).
[13] H. Iwasaki *et al.*, Phys. Lett. B **620**, 118 (2005).
[14] M. Belleguic *et al.*, Phys. Rev. C **72**, 054316 (2005).
[15] Y. Utsuno *et al.*, Phys. Rev. C **60**, 054315 (1999).
[16] M. Labiche *et al.*, Nucl. Inst. Meth. A **614**, 439 (2010).
[17] J. Simpson *et al.*, Acta Phys. Hung. **11**, 159 (2000).
[18] S. Pullanhiotan *et al.*, Nucl. Inst. Meth. A **593**, 343 (2008).
[19] W.N. Catford, Nucl. Phys. A **701**, 1c (2002).
[20] B. Fernández-Domínguez *et al.*, Phys. Rev. C **84**, 011301(R) (1999).
[21] J.M. Lohr and W. Haeberli, Nucl. Phys. A **232**, 381 (1974).
[22] K. Amako, Nucl. Inst. Meth. A **453**, 455 (2000).
[23] S.M. Brown, Ph.D. Thesis, University of Surrey, (2010); http://epubs.surrey.ac.uk/2829/1/thesis.pdf
[24] R.C. Johnson and P.J. Soper, Phys. Rev. C **1**, 976 (1970).
[25] J. Lee *et al.*, Phys. Rev. C **75**, 064320 (2007).
[26] F.D. Becchetti and G.W. Greenlees, Phys. Rev. **182**, 1190 (1969).
[27] R.L. Varner *et al.*, Phys. Rep. **201**, 57 (1991).
[28] H.J. Rose and D.M. Brink, Rev. Mod. Phys. **39**, 306

(1967).
[29] C.M. Vincent and H.T. Fortune, Phys. Rev. C **2**, 782 (1970).
[30] S.G. Cooper *et al.*, J. Phys. G **8**, 559 (1982).
[31] S. Sen *et al.*, Nucl. Phys. A **219**, 429 (1974).
[32] E.K. Warburton and B.A. Brown, Phys. Rev. C **46**, 923 (1992).
[33] B.H. Wildenthal, Prog. Part. Nucl. Phys. **11**, 5 (1984).
[34] F. Meurders and A. van der Steld, Nucl. Phys. A **230**, 317 (1974).
[35] F. Maréchal *et al.*, Phys. Rev. C **72**, 044314 (2005).
[36] see, for example, G. Hagen *et al.*, Phys. Rev. C. **83**, 021305(R) (2011).
[37] Curiously, data from ^{12}C(^{28}Ne,^{27}Neγ) [13] exhibits only the higher energy γ-ray, whilst fragmentation of ^{36}S [14] shows only the lower transition.